Characterization of a Hamamatsu R7600 multi-anode photomultiplier tube with single photon signals

2013 JINST 8 P02012

(http://iopscience.iop.org/1748-0221/8/02/P02012)

JINST

PUBLISHED BY IOP PUBLISHING FOR SISSA MEDIALAB

RECEIVED: *December 3, 2012*
ACCEPTED: *January 25, 2013*
PUBLISHED: *February 20, 2013*

Characterization of a Hamamatsu R7600 multi-anode photomultiplier tube with single photon signals

M. Calvi,[a,b] **A. Giachero,**[a,b] **C. Gotti,**[a,c,1] **M. Maino,**[a,b] **C. Matteuzzi**[a,b] **and G. Pessina**[a,b]

[a]*INFN, Sezione di Milano Bicocca,*
Piazza della Scienza 3, 20126, Milano, Italy
[b]*Dipartimento di Fisica G. Occhialini, Università degli Studi di Milano Bicocca,*
Piazza della Scienza 3, 20126, Milano, Italy
[c]*Dipartimento di Elettronica e Telecomunicazioni, Università degli Studi di Firenze,*
via S. Marta 3, 50139, Firenze, Italy

E-mail: `claudio.gotti@mib.infn.it`

ABSTRACT: The characterization of the single photon response of the Hamamatsu R7600 multi-anode photomultiplier tube (MaPMT) is presented, in view of a possible application in Ring Imaging Cherenkov (RICH) detectors and high rate single photon counting applications in general. For most of the measurements the main source of single photons was a commercial blue LED biased with a small current of a few nA. The spectra obtained with this source match those obtained with Cherenkov light from a PbF_2 crystal illuminated with a ^{22}Na gamma source, confirming that the test signals are single photons. Dark current and cross-talk were measured at the single photoelectron level. The single photon response of the PMT was also studied as a function of the bias ratio between dynodes. The sensitivity to magnetic field up to 30 G and the effectiveness of three magnetic shields with different geometries were evaluated. Gain loss due to aging was also studied up to 2000 hours of operation at high counting rate.

KEYWORDS: Photon detectors for UV, visible and IR photons (vacuum); Detectors for UV, visible and IR photons; Photon detectors for UV, visible and IR photons (vacuum) (photomultipliers, HPDs, others)

---

[1] Corresponding author.

doi:10.1088/1748-0221/8/02/P02012

2013 JINST 8 P02012

Contents

---

1 Application requirements

The Ring Imaging Cherenkov (RICH) detectors of high energy physics experiments such as LHCb [1] allow the identification of charged particles through the measurement of the Cherenkov angle of the light they produce when crossing a properly chosen medium. The Cherenkov light generated by each particle consists of a few tens of photons, which need to be detected with adequate spatial resolution on the photodetector plane. In the case of LHCb RICH detectors the required pixel size is about 2x2 mm^2, depending on the overall layout of the upgraded detector, and the photodetectors should provide single photon detection capability, which calls for negligible cross-talk between neighbouring pixels and negligible dark current with respect to the signal rate. In addition to that, the photodetectors must not be affected by the surrounding magnetic field of up to 30 G (3 mT).

The LHCb upgrade aims at a tenfold increase in luminosity with respect to the current design value and calls for a higher readout speed from all the subdetectors. Currently custom built Hybrid Photon Detectors (HPDs) [2] are employed in the LHCb RICH. The readout speed of the HPDs is limited by the built-in readout chip, which cannot be easily replaced without disassembling the devices. Substituting the HPDs with another kind of photodetector is considered a better option. Multi-anode photomultiplier tubes were chosen as the alternative photodetectors [3, 4]. For this reason, we characterized first the Hamamatsu H9500 [5] and then the R7600 [6] for single photon response. The measurements performed so far on the R7600 are presented in this paper.

The Hamamatsu R7600 has 8x8 anodes of 2 millimeters side each, separated from a pixel border of 0.3 mm, thus providing very good spatial resolution. However, due to the large inactive area near the sides of the PMT, the total active area of this model is only about 50%. If this tube

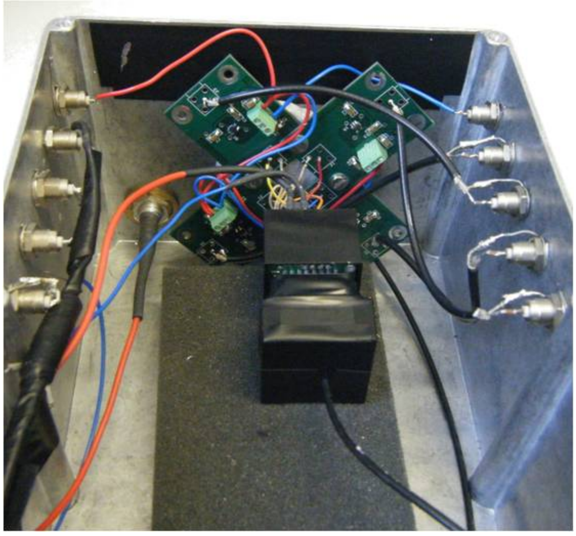

Figure 1. Setup for generating single photon signals, showing the LED on the left (wrapped in black tape), and the optical fiber connecting the LED to a PMT pixel. The four amplifiers are also visible on the back of the PMT.

were to be used in the RICH upgrade, then an optical concentrator would have to be incorporated to increase the geometric efficiency. This does not seem to be the case for a new Ma-PMT model from Hamamatsu, the R11265, which was recently made available. This new PMT is very similar to the R7600 but for the smaller PMT border, for an active area ratio of about 75%.

The R11265 since its release is considered for the LHCb RICH a better candidate than the R7600. Anyway, due to its good performance and lower price compared to the R11265, the R7600 can still be preferrable to the R11265 for all the single photon counting applications where its larger border does not constitute a problem. Since the R11265 is now the baseline for the LHCb upgrade, the studies on the R7600 presented in this paper were performed with a limited statistics of a few devices.

2 Setup for single photon generation

The LED setup for single photon generation is the same as described in [5]: a blue commercial LED biased with a small DC current, of the order of 10 nA, coupled on a side with an optical fiber. Since most of the photons are emitted from the front of the LED, coupling the fiber on the side allows to collect only a small fraction of the generated photons. The other end of the optical fiber was sent directly to a pixel of the PMT, while the neighbouring pixels were covered with a black mask and black tape to prevent light from passing. The illuminated spot is a circle of 1 mm diameter, given by the dimensions of the optical fiber. The spot is centered on the PMT pixel. A cluster of 4 anodes of the PMT, the one under the optical fiber and three of its nearest neighbours, were read out by commercial wide-bandwidth current feedback operational amplifiers (CFOAs) [7]. A picture of the setup is shown in figure 1. The signals at the outputs of the CFOAs were acquired with a Tektronix DPO7254 fast oscilloscope.

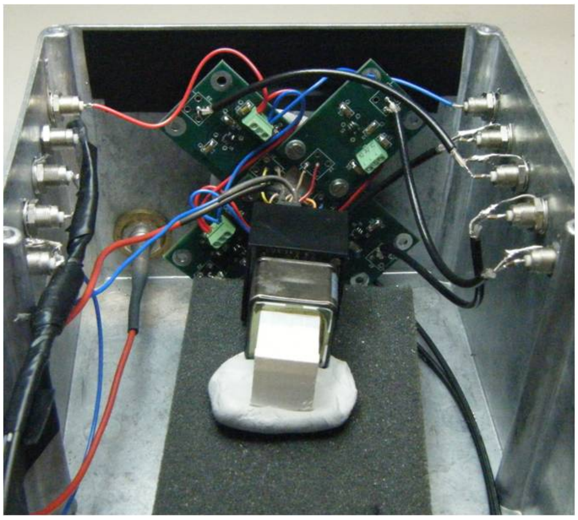

Figure 2. Alternative setup for generating single photon signals, showing the PbF_2 crystal in front of the PMT.

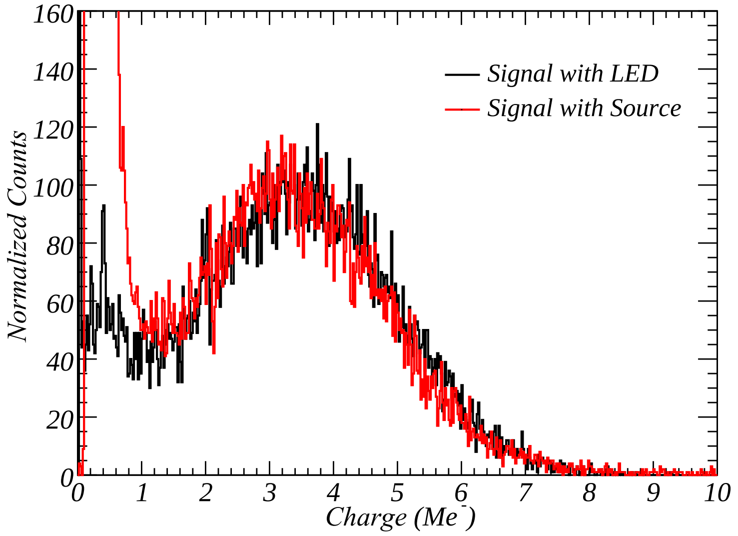

Figure 3. Comparison between the single photon spectra obtained with the two methods described in the text. The spectra are in good agreement in the single photon region, proving that the DC biased LED is a single photon source. The PMT was biased with HV = -950 V with the standard bias voltage ratio from Hamamatsu.

An alternative method was also used to prove the capability of the LED setup to operate in single photon condition. A PbF_2 crystal (n=1.82, ρ=7.7 g/cm^3) [8] was placed in front of the PMT, in a light-tight enclosure. A ^{22}Na source was then placed in front of the crystal. The source emits 511 keV and 1275 keV photons towards the crystal, where electrons are liberated by photoelectric effect and generate Cherenkov photons to be detected by the PMT. This alternative setup is shown

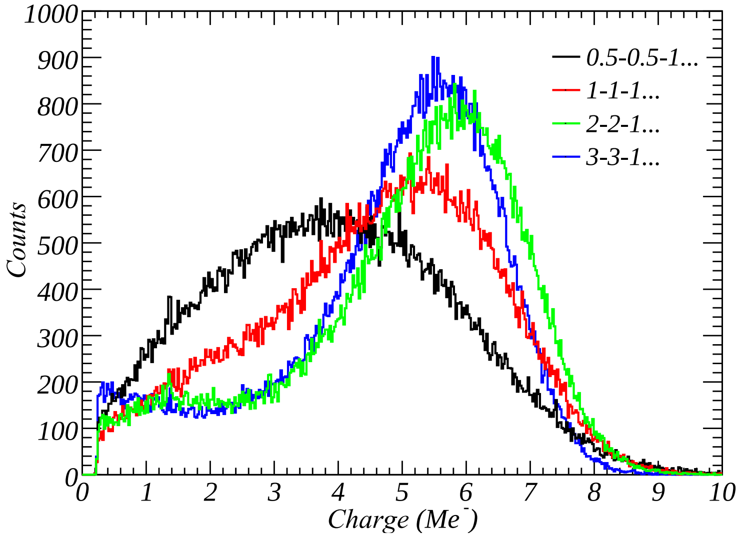

Figure 4. Comparison between spectra with different bias voltage ratios, looking for the best configuration for single photon counting.

in figure 2. The secondary photons are about twenty on average for each decay of the source, and are emitted simultaneously. They are expected to hit different pixels on the PMT, since the crystal is segmented in subsections of about 5 millimeters side, each covering the area of 4 pixels. If the optical coupling between the crystal and the PMT were perfect, we would expect to observe about five photoelectrons per decay, hitting different pixels in coincidence, since the quantum efficiency of the bialkali photocathode is about 25%. However, internal reflection and absorption reduce the number of photons hitting the PMT to one, at most, per decay. The output spectra were acquired and compared with the spectra obtained with the LED setup. Figure 3 shows the two spectra, normalized to the same number of counts in the single photon region. There is a good match in the single photon region, i.e. above 1 Me^-, showing the single photon peak at about 3.5 Me^- in both cases. This provides proof that the DC biased LED setup is capable of single photon generation and detection. The noise pedestal, in the low part of the spectra, differs. Since the pedestal is due to electronic noise coming from the dynodes of the PMT, it depends on measurement conditions and spectra normalization, and is not related to single photon events.

3 Gain and bias

The standard bias socket from Hamamatsu designed for continuous light detection divides the high voltage between dynodes with a 3-2-2-1-...-1-2-5 ratio from the first dynode to the last, and thus gives a larger voltage ratio to the first and last dynodes of the PMT. A larger voltage at the first stages allows to generate larger signals at the first multiplication steps and helps to improve signal to noise ratio in continuous light as well as in single photon counting applications. On the other side a larger voltage at the last dynodes helps to improve the linearity, as long as an analog reading of current from continuous light is of interest. For single photon counting it is unnecessary, on one side because this regime usually draws smaller currents from the anodes than continuous light, and on the other because linearity is not important, since the signal is meant to represent a binary information (if the pixel is hit by a photon or not). The larger bias at the last stages can thus be avoided.

A printed circuit board was designed and built in order to be able to adjust the bias voltage ratio, looking for the best configuration for single photon counting. The single photon spectra for some bias configurations, differing for the voltage ratio at the first two dynodes, are shown in figure 4. The best configuration is found to be at ratios of 2-2-1-...-1 or 3-3-1-...-1, proving that the peak for single photon signal is sharper and is better resolved from noise when the bias of the first two stages is increased with respect to the following stages. The overall bias voltage in these measurements was not constant: it was adjusted by hand in order to obtain the same single photon spectrum endpoint. These spectra should also be compared to the single photon spectrum obtained with the standard Hamamatsu socket, depicted in figure 3. Thus we conclude that a higher ratio at the first two dynodes with respect to all the others best fit single photon counting applications. Since going from 2-2-1-...-1 to 3-3-1-...-1 introduces only a very subtle difference, we did not try higher ratios, not expecting to be able to sharpen the peak anymore.

4 Dark current

When dealing with photon counting applications, a dark current event above the threshold for single photon counting is a false count, indistinguable from the real signals due to the photons hitting the photodetector. In the case of the R7600 the dark current was measured at room temperature by counting the number of events on a pixel above a given threshold in order to riproduce the way in which false counts would be generated. When counting with a very low threshold, about 100 Ke$^-$, dark current events occur at rate of about 5 Hz per pixel. When the threshold is set at 1 Me$^-$, in the valley between the noise pedestal and the single photon peak as in the spectrum of figure 3, the dark current rate drops at 1.6 Hz per pixel, or about 40 Hz/cm^2. This numbers refers to a R7600 with a standard bialkali photocathode. A R7600 with a ultrabialkali photocathode (of larger quantum efficiency, up to 40% according to the datasheet from Hamamatsu) was also measured, showing a dark current of the same order of magnitude.

5 Cross-talk

It was shown in a previous paper on the H9500 Ma-PMT [5] that the cross-talk signal in single photon applications can exceed the continuous light cross-talk specification given in the datasheet, and can be as high as the main signal. This happens if the cross-talk is caused by a few electrons jumping on the neighbouring pixel after the first multiplication stage, an effect which becomes very significant at the single photoelectron level, as was observed in the H9500. This mechanism is also sometimes referred to as charge sharing. In the case of the R7600 this mechanism was not observed, and cross-talk was found to be negligible, well below 1%. This charge sharing effect can only occur after the first multiplication stage, and as such it is not expected to depend on the position of the incoming photon with respect to the pixel border.

Figure 5 shows the oscilloscope traces at the output of the CFOAs for a pixel where about a hundred single photons are sent, and for one of its nearest neighbours. All the neighbouring pixels

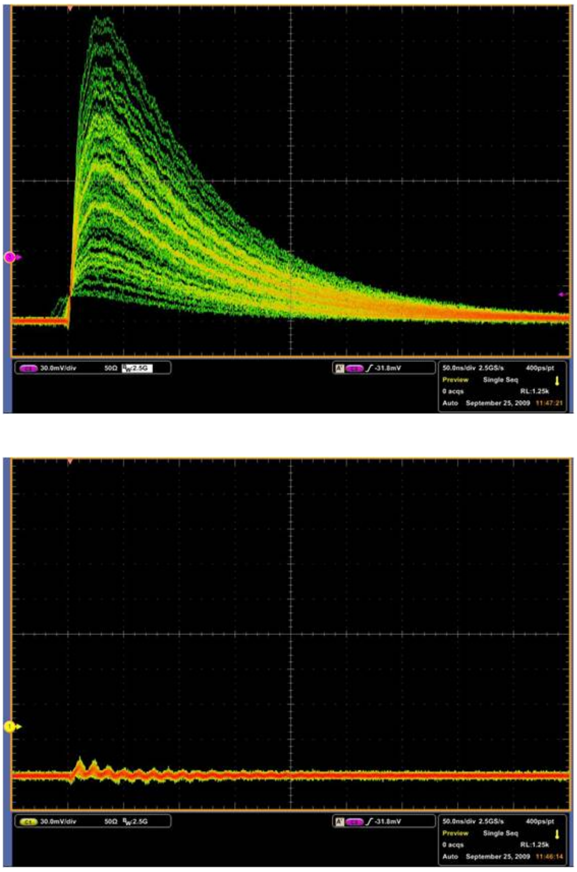

Figure 5. Signals from two neighbouring pixels when single photons are hitting one of them (upper figure), showing negligible cross-talk in the other (lower figure). The horizontal time scale is 50 ns/div.

were measured and gave the same results. It shows clearly that there is no cross-talk at the single photon level. The neighbouring pixels show a small oscillation with a period of about 10 ns which is probably induced through the dynode bias, and it is anyway very low and below threshold in single photon counting applications.

Another possible cross-talk mechanism is the optical cross-talk, which occurs if the single photoelectron generated at the photocathode deviates on a neighbouring pixel before the first dynode. In single photon counting mode, there is only one photoelectron out of the photocathode and entering the multiplication chain. In this case, the photoelectron may deviate and all the signal would be found on the neighbouring pixel, while no signal would be found in the "correct" pixel. This would happen mostly when the photons hit the photocathode near the border between two pixels. This cross-talk mechanism was not measured, since it is expected to be very low from Hamamatsu specifications.

A third possible source of cross-talk is the cross-talk in the readout electronics, which is related to the stray capacitance between the anodes, less than 1 pF. This cross-talk is negligible if the input impedance of the readout chain is low enough, as in our case with CFOAs.

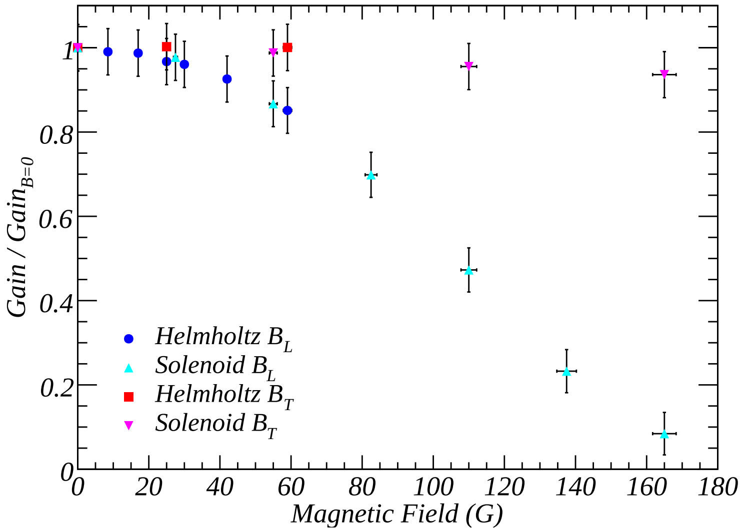

Figure 6. Gain loss due to magnetic field for a pixel near the center of the PMT. Two devices were used to generate the magnetic field, a Helmoltz coil and a solenoid, as described in the text. The axial and transversal fields were indicated by B_L and B_T respectively.

6 Behaviour in a magnetic field

The response of photomultiplier tubes is in general very sensitive to magnetic field. If the R7600 Ma-PMT needs to be deployed in an environment with non negligible values of magnetic field, as often happens in the case of high energy physics detectors, then its gain loss and eventually the crosstalk performance in magnetic field need to be assessed. In the case of the LHCb RICH, for instance, the photodetectors to be employed must be insensitive to the residual magnetic field due to the LHCb dipole of about 30 G (3 mT) for the RICH1, less for the RICH2. This value already takes into account the outer iron shield of the RICH.

The effect of magnetic field on the single photon spectra of the R7600 was measured. To generate the magnetic field for our tests we used two devices, a solenoid capable to generate fields up to 300 G, and a Helmholtz coil for more uniform fields up to about 60 G. The field intensity was measured with a Hirst GM04 gaussmeter.

Figure 6 shows the relative gain loss of a pixel at the center of the PMT versus the magnetic field applied. We found this effect to depend heavily on the field direction with respect to the PMT. For transversal fields, entering the PMT from the side, the effect is neglibile up to 100 G and more. The main reason for this is that the sides of the PMT are in metal and they shield the magnetic field. On the other side, a field whose direction is axial with the PMT, from front to back, causes a significant gain decrease. This is probably due to the field action on the lateral component of the trajectories of the electrons during multiplication, causing them to deviate and fall on less doped regions of the following dynodes, thus reducing the multiplication gain. This effect was found not to depend on the bias voltage, i.e. on electron acceleration induced by the electric field in the multiplication process. This can be interpreted as follows: since the deviation of a charged particle

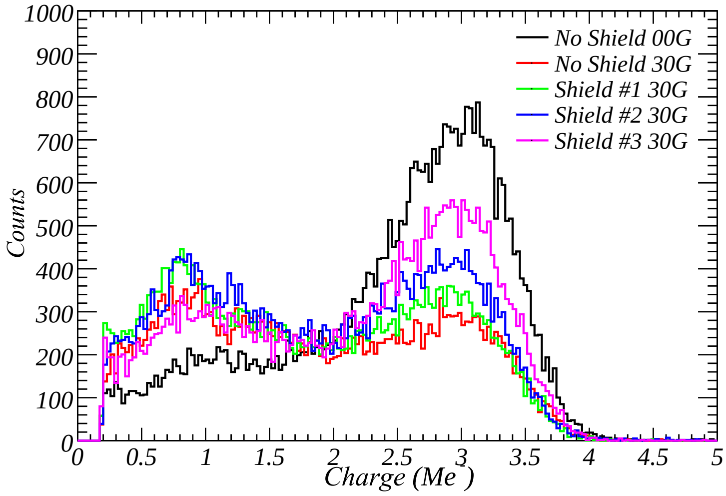

Figure 7. Single photon spectra of a pixel on the border of the PMT for a 30 G axial magnetic field. The PMT was biased with HV = -800 V with the 3-3-1-...-1 bias ratio.

Figure 8. The R7600 Ma-PMT and the three magnetic shields that were tested.

in a magnetic field is higher when the particle is slower, the largest effect of the magnetic field on the trajectories of the electrons occurs when the electrons are slower. This happens right after they come out of each dynode, before they are accelerated by the bias voltage: thus the gain loss is independent of the bias voltage.

The measurements shown in figure 6 were taken on a pixel near the center of the PMT. For these pixels a field up to about 50 G does not cause a significant gain loss. Pixels on the edge on the contrary show a higher sensitivity to magnetic field. In fact without additional shielding the signal loss on a pixel on the edge is already more than 50% for an axial fields of 30 G, as can be seen in figure 7. To preserve the good response on the peripheral pixels additional magnetic shielding is thus advisable. Three shields were applied to the PMT, shown in figure 8. The shields were built with 0.2 mm thick Skudotech®, a high magnetic permeability alloy, similar to Mu-metal®. All shields have the same thickness but differ in shape. The first shield only covered the four sides of the PMT, without protruding over the front or the back of the PMT. The second shield was like the first, but protruding for half a centimeter over the front and back of the PMT. The third shield was like the second, but with an additional part covering the back of the PMT, intersecting the axial field lines. This third shield is similar to the shield used in the upgraded COMPASS RICH, which employs R7600 PMTs, although in the 4x4 pixels version [9]. The effectiveness of these magnetic shields at 30 G can be evaluated in figure 7. While modest improvements can be measured with the first and second shield, only the third succeeds in effectively shielding the peripheral pixels of the PMT.

7 Gain aging

The aging of the tube manifests by two main effects. One is the aging of the photocathode, which can lose quantum efficiency over time, and the other is the aging of the multiplication chain, which causes a gain reduction. Since for single photon counting applications the charge extracted from the photocathode is very low even at high counting rate, the aging of the photocathode is not expected to be significant. The aging of the last dynodes instead will be very significant at high counting rates since the signal after electron multiplication is much larger. The measurement of the gain reduction can be performed with the simple LED setup which was used for all the charaterization described so far [10]. The LED was placed in front of a cluster of five pixels, and was controlled with a Agilent E3631A DC voltage source remotely controlled with a PC. The mean output current from the illuminated pixels was continuously monitored by a Keithley 2700 Multimeter and acquired by the PC every ten minutes. The bias voltage for the LED was adjusted in order to keep the current of the most illuminated pixel constant and equal to 1 μA. This made the system stable with respect to variations in temperature and other environmental conditions which affect the light yield of the LED. About once a week the single photon spectra were acquired and gain was measured. The results are plotted in figure 9. A gain loss of about 60% can be seen in the first 200 hours (one week of continuous operation). Then the gain loss curve flattens, reaching 50% after 1600 hours (two months of continuous operation).

For single photon counting applications, the average output current can be related to the photon counting rate simply by dividing the average current by the mean output charge for single photoelectrons. For instance, assuming the mean single photoelectron signal to be 3.5 Me^- (0.56 pC), as in the the spectra of figure 3, then the current of 1 μA used in the measurements corresponds to a signal rate of about 1 uA / 0.56 pC $\simeq$ 2 MHz, which is not unreasonably high for high rate single photon counting applications. At such rate the gain aging of the R7600 is expected to become noticeable after only about 100 hours of operation. However after the first 500 hours of operation at such rate further aging becomes almost negligible: it is then possible to compensate the initial gain loss with a larger bias voltage ad operate the device at almost constant gain up to at least 2000 hours. If necessary, the PMTs could be operated with a lower bias voltage, lowering the single photoelectron gain, in order to limit the gain loss effect.

8 Conclusions

The Hamamatsu R7600 was characterized for single photon response in view of its possible application for single photon counting applications. The characterization procedure employed a very simple method to generate single photon signals, whose validity was checked by comparison with single Cherenkov photons generated in a PbF_2 crystal. The PMT shows very good single

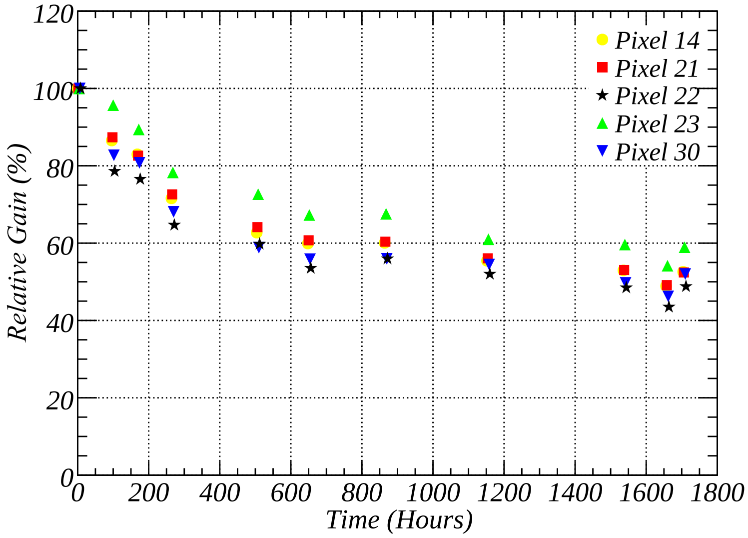

Figure 9. Gain loss due to PMT aging for five pixels of the R7600.

photoelectron resolution, with a negligible rate of dark current and cross-talk. The resolution of the single photon peak can be enhanced by using a custom bias ratio which better fits this application. Measurements in a magnetic field show a gain decrease in presence of axial field components, which becomes critical on pixels near the edges; however a proper magnetic shielding around each PMT solves the problem with fields up to about 30 G. Gain loss due to aging may be significant in high rate photon counting applications, in the MHz range.

Acknowledgments

The authors would like to thank Ezio Previtali and Tommaso Tabarelli De Fatis for the useful ideas and support with the PbF_2 single photon generation setup.

References

[1] LHCb collaboration, *The LHCb detector at the LHC*, 2008 *JINST* **3** S08005.

[2] M. Moritz et al., *Performance study of new pixel hybrid photon detector prototypes for the LHCb RICH counters*, *IEEE Nucl. Sci. Symp. Conf. Rec.* (2003) 986.

[3] LHCb collaboration, *Letter of intent for the LHCb upgrade*, CERN-LHCC-2011-001, CERN, Geneva Switzerland (2011).

[4] LHCb collaboration, *Framework TDR for the LHCb upgrade: technical design report*, CERN-LHCC-2012-007, CERN, Geneva Switzerland (2012) [LHCB-TDR-012].

[5] C. Arnaboldi et al., *Crosstalk study of the single-photon response of a flat-panel PMT for the RICH upgrade at LHCb*, *IEEE Trans. Nucl. Sci.* **57** (2010) 2267.

[6] C. Arnaboldi et al., *Characterization of a Hamamatsu R*7600 *multi-anode photomultiplier tube with single photon signals*, *IEEE Nucl. Sci. Symp. Conf. Rec.* (2010) 1124.

[7] A. Giachero, C. Gotti, M. Maino and G. Pessina, *Current feedback operational amplifiers as fast charge sensitive preamplifiers for photomultiplier read out*, 2011 *JINST* **6** P05004.

[8] E.B. Dally and R. Hofstadter, *A lead fluoride Cerenkov shower counter*, *IEEE Trans. Nucl. Sci.* **15** (1968) 76.

[9] P. Abbon et al., *Design and construction of the fast photon detection system for COMPASS RICH*-1, *Nucl. Instrum. Meth.* **A 616** (2010) 21.

[10] M. Calvi et al., *Aging and time resolution measurements for the Hamamatsu R*7600 *multi-anode photomultiplier tube*, *IEEE Nucl. Sci. Symp. Conf. Rec.* (2011) 1638.

2013 JINST 8 P02012